Left ventricular ejection fraction determined with the simulation of a very low-dose CZT-SPECT protocol and an additional count-calibration on planar radionuclide angiographic data

Hubert Tissot, MD,[a] Véronique Roch, MSc,[b] Olivier Morel, MD,[c] Nicolas Veran, PharmD,[d] Mathieu Perrin, MD,[d] Marine Claudin, MD,[d] Antoine Verger, MD, PhD,[a,e] Gilles Karcher, MD, PhD,[a] Pierre-Yves Marie, MD, PhD,[a,f] and Laetitia Imbert, PhD[b,e,g]

[a] Department of Nuclear Medicine and Nancyclotep Molecular Imaging Platform, CHRU-Nancy, Université de Lorraine, Nancy, France
[b] Department of Nuclear Medicine and Nancyclotep Molecular Imaging Platform, CHRU-Nancy, Nancy, France
[c] CHU-Besançon, Université de Franche-Comté, Service de Médecine Nucléaire, Besançon, France
[d] Department of Nuclear Medicine, CHRU-Nancy, Nancy, France
[e] INSERM, UMR 1254, Université de Lorraine, Nancy, France
[f] INSERM, UMR 1116, Université de Lorraine, Nancy, France
[g] Médecine Nucléaire, Hôpital de Brabois, CHRU-Nancy, Vandoeuvre-Les-Nancy, France

Received Oct 29, 2018; accepted Dec 21, 2018
doi:10.1007/s12350-019-01619-w

Purpose. **To determine whether the left ventricular ejection fractions (EFs), measured on a high-sensitivity CZT single photon emission computed tomography (SPECT)-camera with a 70% reduction in recording times and a prevention of EF overestimation through an additional count-calibration, are concordant with reference EF from planar radionuclide angiography (2D-RNA).**

Methods. **An additional 10-minute CZT-SPECT recording was performed in patients referred to 2D-RNA for cardiomyopathy (n=23) or chemotherapy monitoring (n=50) with an in vivo red blood cell labeling with 850 MBq $^{99m}TcO_4^-$. The EF, obtained from CZT-SPECT with 100% (SPECT100) or 30% (SPECT30) projection times and with a SPECT-count calibration on the 2D-RNA counts of corresponding cavity volumes, were compared to EF from 2D-RNA.**

Results. **Strong and equivalent relationships were documented between the EF from 2D-RNA and the calibrated EF from SPECT100 ($y=0.89x+6.62$; $R^2=0.87$) and SPECT30 ($y=0.87x+8.40$; $R^2=0.85$), and the mean EF from SPECT100 (54%±15%) and SPECT30 (53%±16%) were close to that from 2D-RNA (55%±15%). However, upward shifts in these mean values**

Electronic supplementary material The online version of this article (https://doi.org/10.1007/s12350-019-01619-w) contains supplementary material, which is available to authorized users.

The authors of this article have provided a PowerPoint file, available for download at SpringerLink, which summarises the contents of the paper and is free for re-use at meetings and presentations. Search for the article DOI on SpringerLink.com.

JNC thanks Erick Alexanderson MD, Carlos Guitar MD, and Diego Vences MD, UNAM, Mexico, for providing the Spanish abstract; Haipeng Tang MS, Zhixin Jiang MD, and Weihua Zhou PhD, for providing the Chinese abstract; and Jean-Luc Urbain, MD, PhD, CPE, Past President CANM, Chief Nuclear Medicine, Lebanon VAMC, PA, for providing the French abstract.

Reprint requests: Laetitia Imbert, PhD, MÅdecine NuclÅaire, Hôpital de Brabois, CHU-Nancy, AllÅe du Morvan, 54500 Vandoeuvre-les-Nancy, France; *l.imbert@chru-nancy.fr*

1071-3581/$34.00

were documented in the absence of count calibration for both SPECT100 (60%±18%) and SPECT30 (60%±18%).

Conclusion. **Left ventricular EF may be determined on a high-sensitivity CZT-camera, a 70% reduction in injected activities, and an additional count-calibration for further enhancing the concordance with 2D-RNA values. (J Nucl Cardiol 2019;26:1539–49.)**

Spanish Abstract

Propósito. **Determinar si la fracción de eyección del ventrículo izquierdo, medida con la cámara CZT-SPECT con una reducción del 70% en tiempo de grabación y con la prevención de la sobreestimación mediante una calibración de cuentas adicional, que sea concordante con el valor referencia de fracción de eyección mediante radiografía planar de radionucleidos. (2D-RNA).**

Métodos. **Una grabación adicional de 10 minutos con CZT-SPECT se realizo en pacientes referidos a radiografía planar de radionucleidos (2D-RNA) por miocardiopatías. (n = 23) o para monitorizar las quimioterapias (n = 50) con marcaje de glóbulos rojos con 850 MBq 99m TcO4. La fracción de eyección obtenida por CZT-SPECT con 100% (SPECT100) o 30% (SPECT30) de tiempo de proyección, y con SPECT con calibración de cuentas con el 2D-RNA, los volúmenes de cavidades fueron comparados con fracción de eyección . Relaciones fuertes y equivalentes fueron documentados entre fracción de eyección del 2D-RNA, y la forma calibrada de la fracción de eyección SPECT100 (y = 0.89x + 6.62; R2 = 0.87) y SPECT30 y = 0.87x + 8.40; R2 = 0.85), y la media de fracción de eyección de SPECT100 (54 ± 15%) and SPECT30 (53 ± 16%) fueron cercanos a la de el 2D-RNA (55 ± 15%). Aunque, aumentos en estas medias se documentaron en la ausencia de la calibración de cuentas para SPECT100 (60 ± 18%) y SPECT30 (60 ± 18%).**

Conclusión. **La fracción de eyección del ventrículo izquierdo puede ser determinada con una cámara CZT de alta sensibilidad, una reducción del 70% en actividades inyectadas y la calibración de cuentas adicional para realzar la concordancia con los valores de 2D-RNA. (J Nucl Cardiol 2019;26:1539–49.)**

Chinese Abstract

目的. 以平面放射性核素血管造影 **(2D-RNA)** 测定左心室射血分数 **(EF)** 作为参考标准,为确定利用高灵敏度 **CZT SPECT** 相机在减少 **70%** 的记录时间, 并结合计数校准防止高估情况下测量的 **EF**值, 是否与 **2D-RNA** 测得的 **EF** 值一致。

方法. 对心肌病 **(n = 23)** 或化疗监测 **(n = 50)** 的患者采用体内标记法注射 **850 MBq $^{99m}TcO_4$** 标记的红细胞进行 **2D-RNA** ,随后再采集 **10** 分钟 **CZT-SPECT**。 对 **CZT-SPECT 100%** 投影时间 **(SPECT100)** 或 **30%** 投影时间 **(SPECT30)** 获得的图像进行重建, 并进行计数校准 (对相应容积获得的 **2D-RNA** 计数通过 **SPECT** 校准)获得 **EF** 值, 与 **2D-RNA** 测定的 **EF** 的进行比较。

结果. **2D-RNA** 测定的 **EF** 值与 **SPECT100** 校准后测定的 **EF** 值 **($y = 0.89x + 6.62$; $R^2 = 0.87$)** 及 **SPECT30 ($y = 0.87x + 8.40$; $R^2 = 0.85$)** 校准后 **EF** 值具有高度相关性, 并且 **SPECT100 (54 ± 15%)** 和 **SPECT30 (53 ± 16%)** 测定的 **EF** 平均值与 **2D-RNA** 测定的 **EF** 平均值 **(55 ± 15%)** 非常接近。 但是, 在没有计数校准的情况下, **SPECT100 (60 ± 18%)** 和 **SPECT30 (60 ± 18%)** 测定的 **EF** 平均值会被高估。

结论. 高灵敏度 **CZT** 相机可在减少 **70%** 的注射剂量情况下测定左心室 **EF** 值, 结合计数校准可进一步提高与 **2D-RNA**测得的 **EF** 值的一致性。

关键词: 放射性核素血管造影; 血池 **SPECT; CZT** 相机; 左心室射血分数; 校准曲线。 **(J Nucl Cardiol 2019;26:1539–49.)**

French Abstract

Objectif. **Déterminer si les fractions d'éjection ventriculaire gauche (EF) mesurées sur une caméra CZT SPECT à haute sensibilité avec une réduction de 70% des temps d'enregistrement et une prévention de la surestimation de l'EF grâce à un étalonnage supplémentaire des coups concordent avec les EF de référence obtenues par angiographie scintigraphique planaire (2D-RNA).**

Méthodes. **Un enregistrement CZT-SPECT supplémentaire de 10 minutes a été réalisé chez les patients référés pour évaluation de cardiomyopathie (n=23) ou suivi de chimiothérapie (n = 50) par angiographie scintigraphique planaire (2D-RNA) au globules rouges marqués avec 850 MBq 99mTcO4-. Les EF, obtenues au moyen d'une caméra CZT-SPECT avec 100% (SPECT100) ou**

30% (SPECT30) de temps d'acquisition et avec étalonnage des coups SPECT sur les images 2D-RNA des volumes de cavité correspondants ont été comparés aux EF à partir de 2D-RNA.

Résultats. **une corrélation significative existe entre les EF obtenues par 2D-RNA et les EF étalonnées obtenues par SPECT100 (y = 0,89x + 6,62; R2 = 0,87) et SPECT30 (y = 0,87x + 8,40; R2 = 0,85). Les EF moyennes de SPECT100 (54 ± 15%) et SPECT30 (53 ± 16%) sont similaires à celles obtenues par 2D-RNA (55 ± 15%). En l'absence d'étalonnage de comptage des études SPECT100 (60 ± 18%) et SPECT30 (60 ± 18%), ces valeurs moyennes d'EF sont généralement plus élevées.**

Conclusion. **La fonction ventriculaire gauche peut être déterminée avec une caméra CZT à haute sensibilité, une réduction des activités injectées et un étalonnage supplémentaire des coups pour améliorer la concordance avec les valeurs obtenues par 2D-RNA. (J Nucl Cardiol 2019;26:1539–49.)**

Key Words: Radionuclide angiography · Blood-pool SPECT · CZT-camera · Left ventricular ejection fraction · Calibration curve

Abbreviations	
2D-RNA	Planar radionuclide angiography
EDC	End-diastolic counts
EDV	End-diastolic volume
EF	Ejection fraction
ESC	End-systolic counts
ESV	End-systolic volume
LV	Left ventricle
SPECT	Single photon emission computed tomography
SPECT30	SPECT images reconstructed with only 30% of recorded counts
SPECT100	SPECT images reconstructed with 100% of recorded counts

See related editorial, pp. 1550–1551

INTRODUCTION

Planar equilibrium radionuclide angiography (2D-RNA) has the particularity of providing a count-based measurement of left ventricular (LV) ejection fraction (EF), which is independent of LV shape. It remains currently prescribed in patients with cardiomyopathy and for whom echocardiography and cardiac MRI are contraindicated or have limited performances (poor acoustic window, pacemakers, etc.), and particularly for detecting the toxic cardiac effects of cancer treatments.[1,2] However, most 2D-RNA performed on Anger cameras involve relatively high injected activities, leading to effective doses of nearly 6 mSv,[3,4] a major issue for conducting the serial examinations required in current patient monitoring.[1,2]

This issue could potentially be overcome with high-sensitivity cameras equipped with semiconductor cadmium zinc telluride (CZT) detectors.[5,6] Among the two commercialized cardiac CZT-cameras, the "D-SPECT" provides the highest tomographic count sensitivity, i.e., 7- to 8-fold higher than that of conventional Anger-cameras.[7] Previous studies have already shown that injected doses can be decreased by a factor of 3 for myocardial perfusion images recorded with the D-single photon emission computed tomography (SPECT) along with recording times of no more than 10 minutes.[8–11] However, it is not known whether such drastic dose reduction can also be applied for blood-pool images recorded with the D-SPECT while at the same time providing a sufficiently high concordance in EF measurement to be used as an alternative to 2D-RNA.

The 3D SPECT methods of EF measurement do not require a determination of background counts, a major source of variation in EF measured with 2D-RNA.[12] SPECT methods have the additional advantage of being much less affected by the partial overlapping of the left ventricle (LV) by the left atrium[3,13] and are less subject to intra- and inter-observer variations,[14,15] as compared with the 2D-RNA methods. However, the SPECT methods generally exhibit a higher susceptibility to small patient motions than 2D-RNA[16] and remain significantly impacted by partial volume effects,[17,18] photon attenuation[19,20] and by differences in the LV contour detection algorithm.[21,22]

Count/volume relationships are likely to be more or less influenced by these various interfering factors with the latter potentially playing a role in the shifts in EF values currently documented for SPECT, as compared with 2D-RNA, particularly with regard to SPECT overestimation of the EF setting in the normal range.[3,4,14,21,22] It may be wondered whether these overestimations can be minimized with further corrections through count-calibration curves. A high concordance in EF determination would help to substitute conventional 2D-RNA by a low-dose SPECT procedure in this setting.

In light of the above, the present prospective study was aimed at determining whether the EF provided by the high-sensitivity D-SPECT camera, combined with additional LV count-calibration as well as with the simulation of a drastic 70% reduction in injected doses, are concordant with the EF obtained with conventional 2D-RNA.

MATERIALS AND METHODS

Selection of the Study Population

The study patients were prospectively selected among those routinely referred to our department for an EF measurement with conventional 2D-RNA in the setting of: (1) a known cardiomyopathy or (2) the monitoring of a cardiotoxic cancer treatment. Patients with significant arrhythmia or an unstable clinical state were excluded, and inclusion was additionally dependent on patient approval and on availability of camera and staff.

According to the study protocol, a blood-pool recording with the D-SPECT was scheduled immediately after the 2D-RNA recording. All study subjects gave signed informed consent to participate, and the study protocol was approved by the local Ethics Committee (CPP Agreement n°13.06.04) and registered on the ClinicalTrials.gov site (NCT02869308).

Recording and Analysis of Conventional 2D-RNA

Red blood cells were labeled in vivo with the intravenous injection of 850 MBq of $^{99m}TcO_4^-$, 20-30 minutes after an initial injection of approximately 6 mg of stannous pyrophosphate. Five to 15 minutes later, the patients were imaged using an E-Cam™ gamma camera (Siemens, Knoxville, Tennessee, USA) equipped with a low-energy high-resolution collimator. Images were recorded in an optimal septal view (left anterior oblique orientation) and according to the following: a ^{99m}Tc energy photopeak [140 keV (±7.5%)], a 10%-20% temporal window, and a pre-count protocol targeted at 8 million counts. Images were displayed into 16 frames per R–R interval, 64 × 64 matrices and squared voxels of 3.56 × 3.56 mm^2.

The EF was calculated with a conventional count-based method on an E.soft workstation (Siemens, Knoxville, Tennessee, USA) and a software providing a fully automatic drawing of the left ventricular regions of interest (ROI), with the background ROI being positioned a few pixels away from the LV inferior-lateral region at end-systole. Manual corrections were applied only in the rare cases of evident errors in the automatic ROI delineation process.

Effective doses were calculated with the ratio of 7.0×10^{-3} mSv·MBq of injected Tc-99m[23] according to the activity measured within the syringe prior to $^{99m}TcO_4^-$ injection with a dedicated dose calibrator (CRC®-15R, Capintec, Inc., Ramsey, NJ, USA).

Recording and Analysis of CZT-SPECT

A 10-minute CZT-SPECT recording was initiated a few minutes after the completion of the 2D-RNA recording and with a comparable method to that used for myocardial perfusion imaging performed with this camera.[8–11] Briefly, patients were set in a semi-reclining prone position with ECG leads pasted in the back, and projections recorded with a 'region-centric' acquisition which maximizes counts arising from a heart area previously defined on a short pre-scan acquisition. A specific algorithm of iterative reconstruction was used to compensate for the loss in spatial resolution of the collimator.

This reconstruction process was applied in this instance not only on the overall projection durations (SPECT100) but additionally on the initial 30% and thus with a 70% count reduction (SPECT30), both of which were performed using the following parameters: 16-interval frames, 4 iterations, 32 subsets, Kernel and Gaussian filters of respectively 0.125 and 5-mm and a 128 × 128 matrix, leading to a voxel size of 4.92 × 4.92 × 4.92 mm^3. LV volume and EF were determined using the count-based method of the Quantitative Blood Pool software (Cedars-Sinai Medical Center).[24] Manual displacements of LV limits were applied for evident errors in the automatic contouring process.

Calibration Curves

Standards were obtained with an inflatable balloon of an almost spherical form filled with an increasing volume of a water solution containing 0.06 MBq·mL^{-1} of ^{99m}Tc and placed in a diffusing environment, at the center of a cylindrical container of 20.4 cm diameter and 20 cm height. This container was filled with a solution containing a 4-fold lower activity concentration of ^{99m}Tc (0.25 MBq·mL^{-1}), a ratio in the range of those currently documented for cavity/background counts on blood-pool SPECT.[13] The experimental device is shown in a Supplemental Figure.

The balloon with its container was placed at the center of the field-of-view of each camera, for 1-2-minute consecutive recordings with increasing balloon volumes ranging from 32 to 400 mL. An artificial pacing rate was set at 60 min^{-1} and the recording and reconstruction parameters were identical to those already described above for patient imaging.

A calibration curve was thereafter completed for the D-SPECT counts with regard to the E-Cam counts documented at the same balloon volumes with: (1) the balloon count values obtained with the software and methods already described above for the patient study and (2) a subsequent count normalization for each camera, to a measured activity level of 1 count unit·mL^{-1} at the highest volume point of 400 mL. The counts from this highest volume are likely to be less affected by interfering factors, especially with regard to the imperfections in the determination of background counts for 2D-RNA and in the delineation of cavity borders for both techniques (algorithms of contour detection, partial volume effects, etc.).

Additional curves were plotted between normalized values of end-systolic counts (ESCs) calculated with the patients' EF from SPECT30, SPECT100 and 2D-RNA. These ESC were estimated with the formula: (1 − EF) × EDC, where EF corresponds to native EF values and EDC to end-diastolic counts. However, EDC was additionally considered to correspond to the absolute value of the end-diastolic volume (EDV) provided by the geometric area-based method of the QBS software.[24] In this manner, counts were normalized to 1 unit·mL^{-1} of cavity volume at end-diastole, similarly to that for the normalization applied to the higher volume in the balloon experiment (see previous paragraphs). In addition, since EDV

may not be directly measured with 2D-RNA, the EDV from SPECT100 or SPECT30 was used for the computing of ESC with the EF from RNA, before being correlated with the corresponding ESC obtained with SPECT100 and SPECT30 respectively.

Representative D-SPECT and 2D-RNA images of the balloon and of a patient, with the associated ROIs and contours, are displayed in Figure 1.

Additional Correction of EF Values

The normalized ESC values, obtained as detailed above with the D-SPECT, were replaced by the corresponding 2D-RNA values from the calibration curves by using the regression equation from Figure 2A. Lastly, these corrected ESC values were used to correct EF via the equation: EF=1 − (ESC/EDC).

Statistical Analysis

Continuous variables are reported as mean±SD and categorical variables, as percentages. The EFs obtained with SPECT100, SPECT30, and 2D-RNA were compared pairwise with paired Student's *t* tests, linear regression analyses and Bland-Altman plots, after controlling for normal distributions of variables and of regression residuals. Unpaired comparisons were performed under the same conditions with Student's *t* tests for continuous variables and with χ^2 tests for categorical variables. A *P* value<.05 was considered to reflect a significant difference.

RESULTS

Calibration Curves

As detailed in Figure 2A, a relatively precise fit was obtained with a linear function for the curve expressing the 2D-RNA counts relative to the D-SPECT counts documented for the same balloon volumes (R^2=0.997). This curve yielded evidence of an underestimation of SPECT counts with an intercept at zero SPECT counts for a residual activity corresponding to a 8.5 mL volume (red arrow in the lower panel of Figure 2). For an upper volume level of 450 mL, this estimation of volume underestimation was close to 7 mL.

As detailed in Figure 2B, this volume shift could be confirmed through the normalized ESCs calculated with the EF from 2D-RNA, SPECT100, and SPECT30. The intercepts at zero SPECT counts were documented for residual 2D-RNA counts corresponding to residual volumes of 9 and 7 mL for SPECT100 and SPECT30, respectively (Figure 2B).

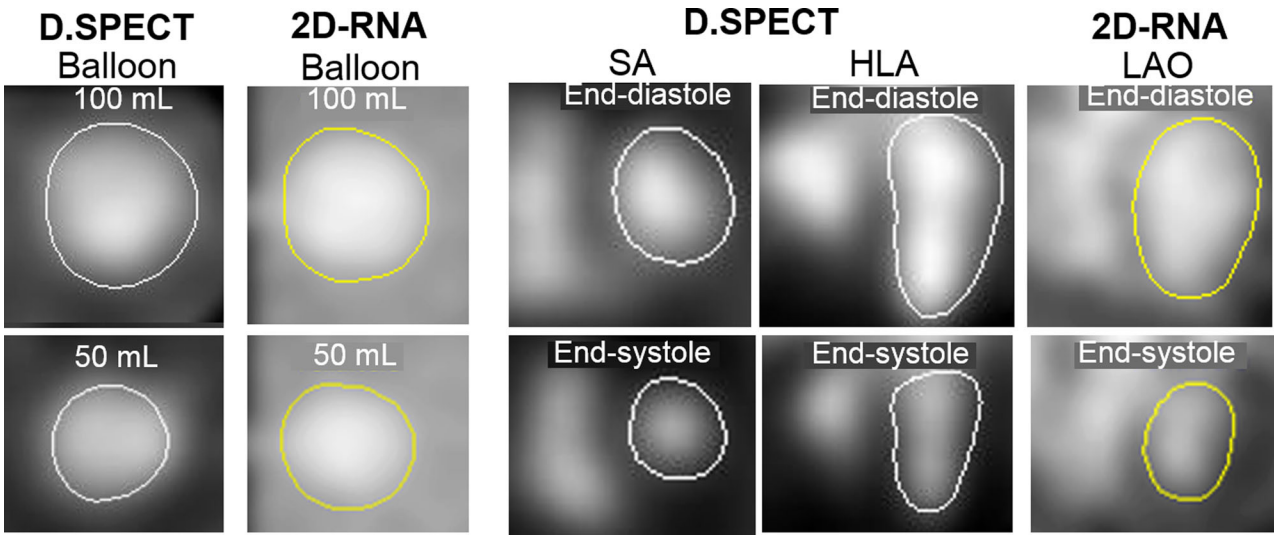

Figure 1. Examples of LV contours obtained on D-SPECT and 2D-RNA images from the balloon filled with solutions of 100 and 50 mL (left panel) and from a patient (right panel). The counts from the 50 mL balloon represented 50% and 45% of the 100 mL balloon counts with 2D-RNA and D-SPECT respectively. The patient EF values were of 61% with 2D-RNA but of 76% and 75% with respectively SPECT100 and SPECT30 in the absence of any SPECT-count calibration, and 66% for both SPECT100 and SPECT30 when using this calibration. *LAO*, left anterior oblique orientation; *SA*, short-axis; *HLA*, horizontal long-axis.

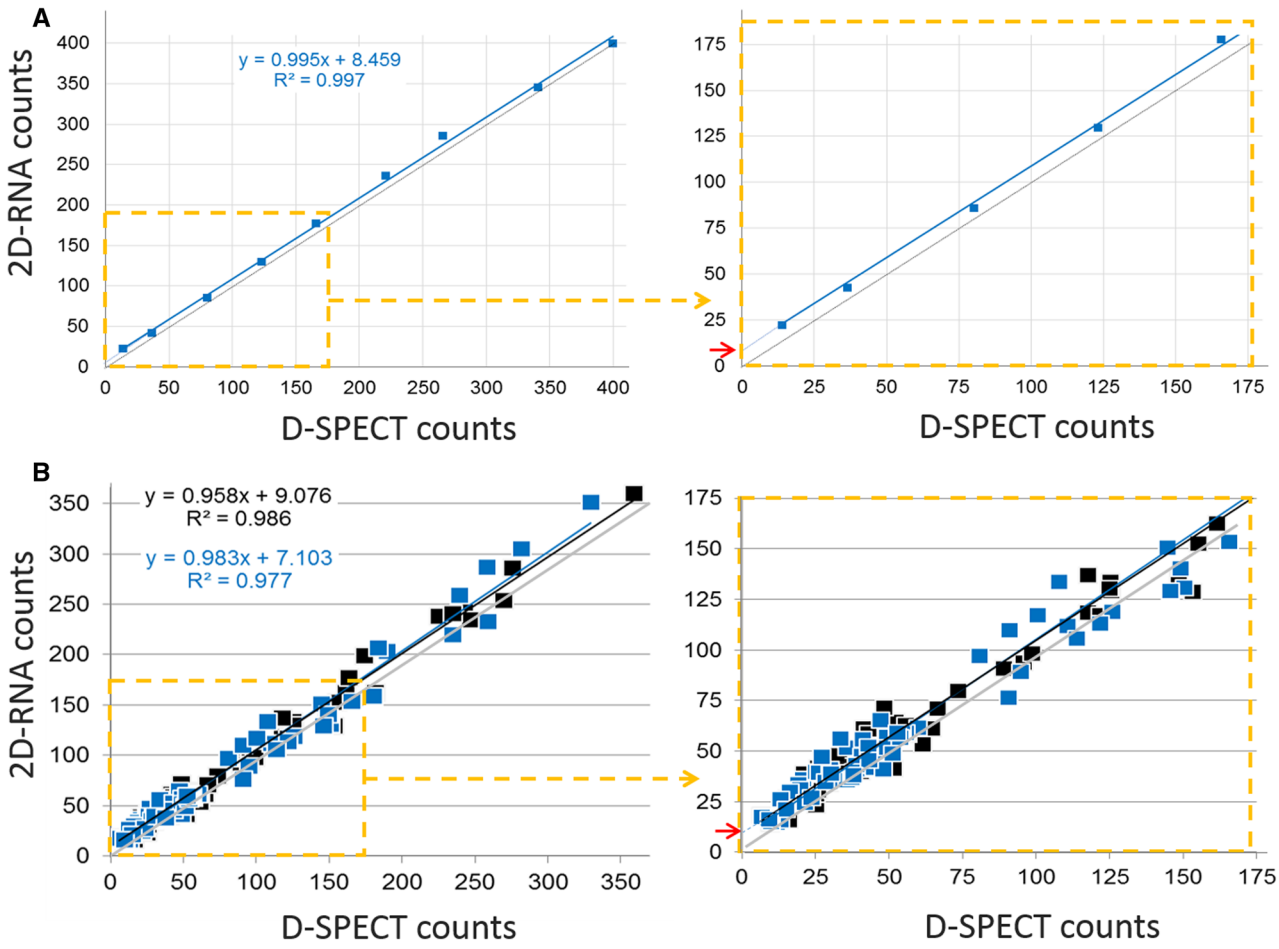

Figure 2. (**A**) 2D-RNA counts values relative to D-SPECT counts at the same volume values, after a normalization for each camera at 1 count unit·mL^{-1} at the 400 mL volume point (and thereby with the same absolute values for counts and volume at this volume point); and (**B**) estimated 2D-RNA end-systolic counts obtained after a normalization at 1 count unit·mL^{-1} of end-diastolic volume from patients (and thereby with the same absolute values for counts and volume at end-diastole) and expressed relative to the corresponding values provided by SPECT100 (black squares) and SPECT30 (blue squares). See text for further details on the methods and note that the intercepts of the linear regressions at a null SPECT counts correspond to volumes ranging between 7 and 9 mL (red arrows).

Patient Characteristics

A total of 73 patients were finally included and the indication for EF determination with 2D-RNA was a known cardiomyopathy in 23 instances (16 ischemic, 5 primitive and 1 valvular cardiomyopathies, and 1 myocarditis) or the monitoring of chemotherapy in the absence of any previously known cardiac disease in the 50 remainders.

The mean age of the overall population was 59±13 years, 66% were women, and as detailed in Table 1, patients from the chemotherapy group were younger and featured a higher proportion of women, a lower body weight and a higher EF at 2D-RNA, as compared with those from the cardiomyopathy group.

Patient Blood-Pool Parameters

On average, total effective dose was 5.9±0.2 mSv and recording time was 16±4 minutes for 2D-RNA and fixed at 10 minutes for the D-SPECT.

The EF levels, obtained after additional count-calibration with SPECT100 (54%±15%) and SPECT30 (53%±16%), were close to those from 2D-RNA (55%±15%), although trends toward lower values were documented in the paired comparisons of the EF from SPECT30 (P=.05) and SPECT100 (P=.10) to those

Table 1. Main patient characteristics in the overall study population and in the cardiomyopathy and chemotherapy groups

	Overall (n = 73)	Cardiomyopathy (n = 23)	Chemotherapy (n = 50)
Age (years)	59 ± 13	65 ± 10	55 ± 13*
Women	48 (66%)	4 (17%)	44 (88%)*
Body weight (kg)	73 ± 16	79 ± 18	70 ± 15*
Body mass index ($kg \cdot m^{-2}$)	26 ± 5	27 ± 4	26 ± 6
Injected activity (MBq)	842 ± 34	832 ± 34	847 ± 34
Effective dose (mSv)	5.9 ± 0.2	5.8 ± 0.2	5.9 ± 0.2
EF values from 2D-RNA (%)	55 ± 15	38 ± 12	63 ± 8*
>50%	52 (71%)	5 (22%)	47 (94%)*
End-diastolic volume (mL)†	168 ± 85	267 ± 73	123 ± 30*
Corrected end-systolic volume (mL)‡	88 ± 76	47 ± 25	177 ± 74

*$P < .05$ for comparisons between the chemotherapy and cardiomyopathy groups
†Obtained with SPECT100 images and the area-based geometric method of QBS software
‡Obtained with SPECT100 images and after correction according to count calibration

from 2D-RNA. Upward shifts in these levels were however documented in the absence of any count calibration, for both SPECT100 (60% ± 18%) and SPECT30 (60% ± 18%; $P < .001$ for the comparisons of SPECT100 or SPECT30 vs 2D-RNA). Hence, the mean EF provided by the D-SPECT before any count calibration exhibited an absolute increase of almost 5%, as compared with the mean EF from 2D-RNA. This absolute increase rose to 7% in the patients with normal EF at 2D-RNA (>50%).

As evidenced in Figure 3, strong and equivalent relationships were documented between the EF from 2D-RNA and the corresponding calibrated values from SPECT100 ($y = 0.89x + 6.62$; $R^2 = 0.87$) and SPECT30 ($y = 0.87x + 8.40$; $R^2 = 0.85$).

Figure 3 also shows that there were similar correlation levels with the EF from 2D-RNA for the non-calibrated SPECT EF as those obtained with the calibrated SPECT EF. However, on the Bland-Altman plots from the same Figure, it may be observed that for averaged D-SPECT/RNA values of more than 50%, the non-calibrated SPECT EF, but not the calibrated SPECT EF, were clearly higher and likely overestimated, as compared with the reference EF values from 2D-RNA.

Finally, as detailed in Figure 4, the calibrated EF values from SPECT30 and SPECT100 were very well correlated between each other ($R^2 = 0.95$), with a 95% confidence interval ranging from − 7.6% to 6.9% for the difference between these two measurements. A high correlation was also documented between SPECT30 and SPECT100 for the EDVs measured with the geometric surface-based method of the QBS software ($R^2 = 0.93$, see Figure 4).

DISCUSSION

The present study shows that an up to 70% reduction in recording times can be applied for count-based EF measurements performed on the very high-sensitivity D-SPECT camera and with a relatively high concordance with the reference 2D-RNA values. However, this concordance was conditioned by the use of a count calibration in order to (i) correct for the underestimation of SPECT counts, a major issue for small LV volumes, and ultimately (ii) prevent from an upward shift in EF values, especially for patients setting in the normal range (i.e., with an EF>50% at 2D-RNA). In the absence of such calibration, the mean EF from the D-SPECT exhibited an absolute increase of almost 7% as compared with that from 2D-RNA in patients setting in the normal EF range.

The patients setting within the normal EF range represented as much as 71% of the present study population, mainly corresponding to those referred to an RNA-based cardiac monitoring of chemotherapy treatment (Table 1). In this current indication,[1,4] where serial RNA exams are needed in addition to other irradiative procedures (oncologic irradiative imaging and/or radiotherapy), a 70% reduction in dose would more than likely be most advantageous. The mean effective dose was 5.9 mSv in our patients, corresponding to that currently documented with 2D-RNA recorded on Anger

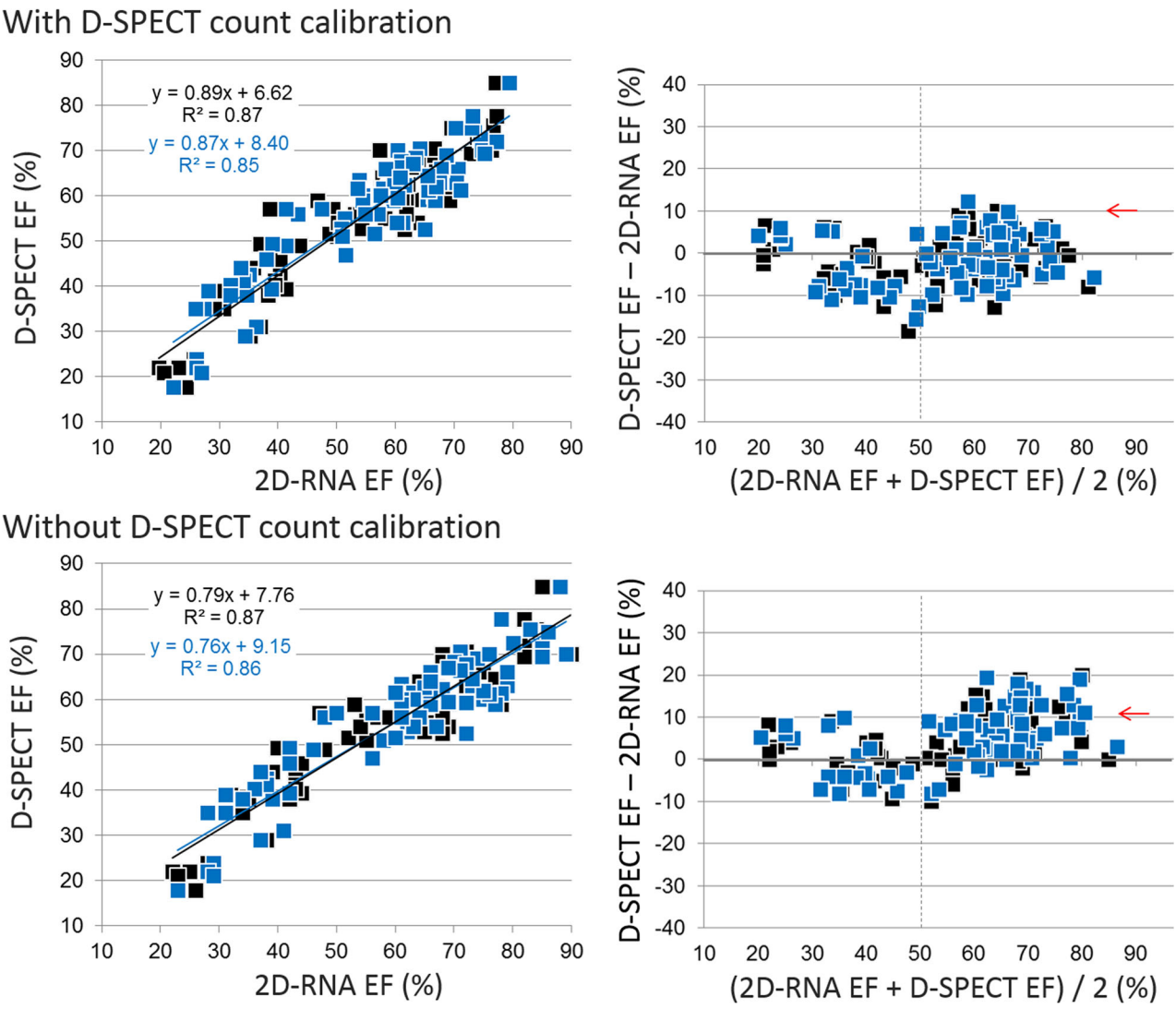

Figure 3. Regression analyses with the EF from 2D-RNA (on the left) and corresponding Bland-Altman plots (on the right) for the EF obtained with SPECT100 (black squares) and SPECT30 (blue squares), both with the calibration of SPECT counts (upper panel) and without this calibration (lower panel). Note that the Bland-Altman analyses yield evidence that the non-calibrated EF values falling in the normal range, contrary to the calibrated EF values, are markedly higher than the corresponding 2D-RNA values (see red arrows).

cameras,[3,4] and in which a 70% reduction would lead to a drastic reduction to a mean value of 1.8 mSv.

Further prospective studies are required to fully assess such low-dose SPECT examinations, especially for identifying an EF falling under the 50% level, as well as an absolute EF decrease of more than 10%, these two criteria being currently used for detecting the toxic cardiac effects of oncologic treatments.[1] However, in previous blood-pool CZT-SPECT studies, the reproducibility and repeatability of EF measurements were already found to be sufficiently propitious for this purpose.[14,15] This consideration is strengthened in the present study by the relatively small difference observed between the two EF measurements obtained with 30% and 100% of SPECT recorded times (Figure 4), along with a 95% confidence interval ranging from − 7.6% to +6.9%.

The observation that current injected activities may be decreased by a factor of 3 or more with the D-SPECT is not surprising since similar results were previously achieved and further validated for patients routinely referred for myocardial perfusion SPECT with this

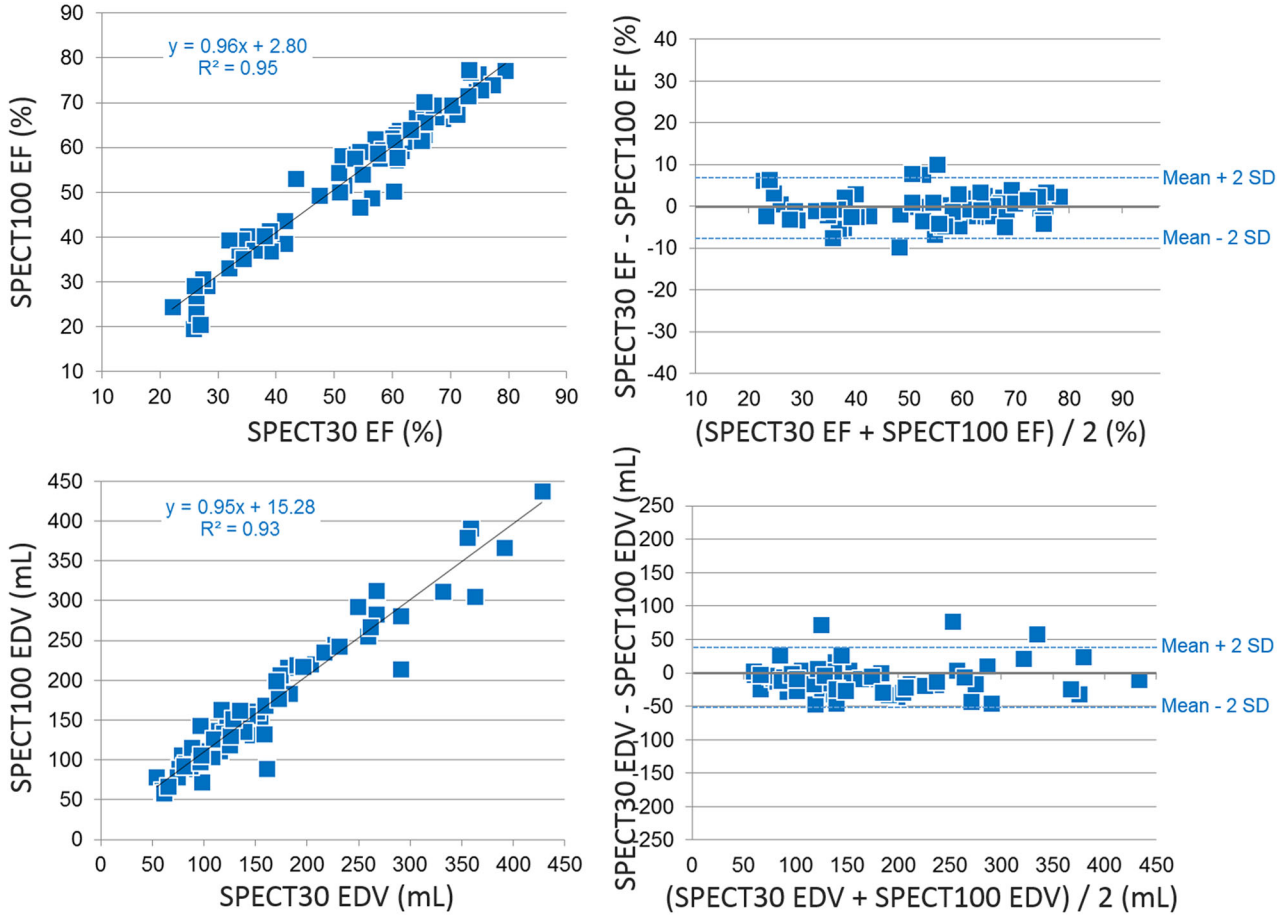

Figure 4. Regression analyses between SPECT100 and SPECT30 (on the left) and corresponding Bland-Altman plots (on the right) for the EF values obtained from the calibrated count-based method (upper panels) and for the end-diastolic volumes (EDVs) obtained with the geometric area-based method of the QBS software. The upper and lower limits of the 95% confidence interval of the difference between the SPECT30 and SPECT100 values have been inserted in the Bland-Altman plots.

camera.[7–11] The tomographic count sensitivity of the D-SPECT was indeed previously shown to be 7-fold higher than that of a current dual-head Anger camera equipped with high-resolution parallel-hole collimators.[7] Notwithstanding the above, the determinations of EF are associated with particular limitations and conditions, which moreover are not exactly the same with planar and SPECT images. In the present study, we hypothesized that the impact of certain potentially confounding factors could be minimized with supplementary corrections through counts calibration curves.

Calibration curves are also currently used for in vitro gamma counters, as well as in analytical chemistry and necessitate to be accurately fitted. Relatively fine fits were obtained in the present study through simple experiments with an inflated balloon placed in a diffusing environment and by using a linear function for the curve matching the D-SPECT counts with the counts provided at the same volume levels by the reference 2D-RNA technique (Figure 2). This latter approach yielded evidence of a constant underestimation of SPECT counts corresponding to 7.0-8.5 mL of cavity volumes.

It may be pointed out that the magnitude of this volume shift could be subsequently confirmed on the end-systolic LV volumes obtained from our patients and by using the uncorrected native EF values from 2D-RNA, SPECT100, and SPECT30 (Figure 2B). The intercepts at zero SPECT counts were found to correspond to a level of residual 2D-RNA volume close to that of the 8.5 mL from the calibration curve—i.e., 9 and 7 mL for SPECT100 and SPECT30 respectively.

The impact on EF measurement of such a 7-9 mL underestimation of the end-systolic volume (ESV) is likely negligible for high LV volumes, such as those documented in our cardiomyopathy group (Table 1). However, this impact is likely much more significant for patients with small LV volumes, such as those from our chemotherapy group (Table 1).

The mechanism of this relative count underestimation remains a matter of debate, presumably involving certain characteristics of the QBS algorithm of LV contouring,[21,22] as well as factors known to affect SPECT counts, such as partial volume effects[17,18] and photon attenuation.[19,20]

From a methodological standpoint, EF values were determined herein with count-based methods, and were subsequently used for the further computing of ESVs. However, counts were additionally normalized at 1 unit·mL^{-1} for the higher volumes (i.e., for the larger balloon and for the LV EDVs of patients). In this manner, the relative underestimation of LV counts by SPECT at end-systole, which is likely the cause of EF overestimation, could be put in relation with a level of volume underestimation (7-9 mL herein).

From a practical standpoint, EF overestimation was suppressed after additional correction based on count-calibration curves and on a rough estimate of EDV provided by the area-method of the QBS software.[25,26] However, it should be emphasized that the use of our balloon-based calibration method is not essential for this purpose. As evidenced in Figure 2B, a simple paired comparison of SPECT and RNA data from the same patients is indeed sufficient for determining the constant volume, which needs to be added to correct for the underestimation of ESVs from the D-SPECT (7-9 mL herein). A dozen patients, with normal or supra-normal EF values, might constitute a sufficiently high sampling for this determination.

In conclusion, this study shows that a 70% reduction in recording times and also presumably in injected activities, can be applied for count-based EF measurements performed on a high-sensitivity CZT-camera and with a relatively good concordance with reference values from 2D-RNA, but at the condition of a supplementary calibration of SPECT counts based on 2D-RNA data.

NEW KNOWLEDGE GAINED

(1) An as much as 70% reduction in injected activities can be applied for the count-based EF measurements performed on a high-sensitivity CZT-camera and (2) the concordance with reference values from 2D-RNA may be enhanced through a supplementary calibration of SPECT counts based on 2D-RNA data.

Acknowledgments

The authors thank Nathaniel Roth and Rafael Baavour from Spectrum Dynamics Medical for their technical support and Pierre Pothier for critical review of the manuscript.

Disclosure

The authors declare that they have no conflict of interest.

References

1. Alvarez JA, Russell RR. Cardio-oncology: The nuclear option. Curr Cardiol Rep. 2017;19:31.
2. Curigliano G, Cardinale T, Suter T, et al. Cardiovascular toxicity induced by chemotherapy, targeted agents and radiotherapy: ESMO clinical practice guidelines. Ann Oncol. 2012;23:vii155–66.
3. Duvall WL, Guma-Demers KA, George T, Henzlova MJ. Radiation reduction and faster acquisition times with SPECT gated blood pool scans using a high-efficiency cardiac SPECT camera. J Nucl Cardiol. 2016;23:1128–38.
4. Hesse B, Lindhardt TB, Acampa W, et al. EANM/ESC guidelines for radionuclide imaging of cardiac function. Eur J Nucl Med Mol Imaging. 2008;35:851–85.
5. Chen YC, Ko CL, Yen RF, et al. Comparison of biventricular ejection fractions using cadmium–zinc–telluride SPECT and planar equilibrium radionuclide angiography. J Nucl Cardiol. 2016;23:348–61.
6. Rydberg J, Andersen J, Haarmark C, Zerahn B. The influence of anthropometric and basic circulatory variables on count rate in cadmium–zinc–telluride SPECT gated radionuclide angiography. J Nucl Cardiol. 2018. https://doi.org/10.1007/s12350-018-1402-9.
7. Imbert L, Poussier S, Franken PR, et al. Compared performance of high-sensitivity cameras dedicated to myocardial perfusion SPECT: A comprehensive analysis of phantom and human images. J Nucl Med. 2012;53:1897–903.
8. Perrin M, Djaballah W, Moulin F, et al. Stress-first protocol for myocardial perfusion SPECT imaging with semiconductor cameras: High diagnostic performances with significant reduction in patient radiation doses. Eur J Nucl Med Mol Imaging. 2015;42:1004–11.
9. Verger A, Imbert L, Yagdigul Y, et al. Factors affecting the myocardial activity acquired during exercise SPECT with a high-sensitivity cardiac CZT camera as compared with conventional Anger camera. Eur J Nucl Med Mol Imaging. 2014;41:522–8.
10. Claudin M, Imbert L, Djaballah W, et al. Routine evaluation of left ventricular function using CZT-SPECT, with low injected activities and limited recording times. J Nucl Cardiol. 2018;25:249–56.
11. Imbert L, Roch V, Merlin C, et al. Low-dose dual-isotope procedure planed for myocardial perfusion CZT-SPECT and assessed through a head-to-head comparison with a conventional single-isotope protocol. J Nucl Cardiol. 2018. https://doi.org/10.1007/s12350-017-0914-z.
12. Tonge CM, Fernandez RC, Harbinson MT. Commentary: current issues in nuclear cardiology [commentary]. Br J Radiol. 2008;81:270–4.
13. Bartlett ML, Srinivassan G, Baker WC, Kitsiou AN, Dilsizian V, Bacharach SL. Left ventricular ejection fraction: Comparison of results from planar and SPECT gated blood pool studies. J Nucl Med. 1996;37:1795–9.
14. Jensen MM, Schmidt U, Huang C, Zerahn B. Gated tomographic radionuclide angiography using cadmium–zinc–telluride detector

gamma camera; comparison to traditional gamma cameras. J Nucl Cardiol. 2014;21:384–96.
15. Jensen MM, Haase C, Zerahn B. Interstudy repeatability of left and right ventricular volume estimations by serial-gated tomographic radionuclide angiographies using a cadmium–zinc telluride detector gamma camera. Clin Physiol Funct Imaging. 2015;35:418–24.
16. Djaballah W, Muller MA, Bertrand AC, et al. Gated SPECT assessment of left ventricular function is sensitive to small patient motions and to low rates of triggering errors: A comparison with equilibrium radionuclide angiography. J Nucl Cardiol. 2005;12:78–85.
17. Nakajima K, Okuda K, Nyström K, et al. Improved quantification of small hearts for gated myocardial perfusion imaging. Eur J Nucl Med Mol Imaging. 2013;40:1163–70.
18. Bailliez A, Lairez O, Merlin C, et al. Left ventricular function assessment using 2 different cadmium–zinc–telluride cameras compared with a γ-camera with cardiofocal collimators: Dynamic cardiac phantom study and clinical validation. J Nucl Med. 2016;57:1370–5.
19. Slart RH, Tio RA, Zeebregts CJ, Willemsen AT, Dierckx RA, De Sutter J. Attenuation corrected gated SPECT for the assessment of left ventricular ejection fraction and volumes. Ann Nucl Med. 2008;22:171–6.
20. Sibille L, Bouallegue FB, Bourdon A, Mariano-Goulart D. Influence of CT-based attenuation correction in assessment of left and right ventricular functions with count-based gated blood-pool SPECT. J Nucl Cardiol. 2011;18:642–9.
21. De Bondt P, De Winter O, De Sutter J, Dierckx RA. Agreement between four available algorithms to evaluate global systolic left and right ventricular function from tomographic radionuclide ventriculography and comparison with planar imaging. Nucl Med Commun. 2005;26:351–9.
22. Harel F, Finnerty V, Ngo Q, Gregoire J, Khairy P, Thibault B. SPECT versus planar gated blood pool imaging for left ventricular evaluation. J Nucl Cardiol. 2007;14:544–9.
23. Cousins C, Miller DL, Bernardi G, et al. ICRP publication 120: Radiological protection in cardiology. Ann ICRP. 2013;42:1–125.
24. Van Kriekinge SD, Berman DS, Germano G. Automatic quantification of left ventricular ejection fraction from gated blood pool SPECT. J Nucl Cardiol. 1999;6:498–506.
25. Harel F, Finnerty V, Grégoire J, et al. Gated blood-pool SPECT versus cardiac magnetic resonance imaging for the assessment of left ventricular volumes and ejection fraction. J Nucl Cardiol. 2010;17:427–34.
26. Xie BQ, Tian YQ, Zhang J, et al. Evaluation of left and right ventricular ejection fraction and volumes from gated blood-pool SPECT in patients with dilated cardiomyopathy: Comparison with cardiac MRI. J Nucl Med. 2012;53:584–91.